Distribution of Tropical Tropospheric Ozone Determined by the Scan-Angle Method applied to TOMS Measurements

Jae H. Kim[1], Sunmi Na[1], and M. J. Newchurch[2], and L. Emmons[3]

1 Department of Atmospheric Science, Pusan National University, Korea

2 Department of Atmospheric Science, University of Alabama in Huntsville, USA

3 Division of Atmospheric Chemistry, NCAR, Boulder, Colorado, USA

Corresponding author address: Jae H. Kim, Department of Atmospheric Science,
Pusan National University, Pusan 609-735, Korea
(E-mail) jaekim@pusan.ac.kr

Abstract

This study introduces the first method that determines tropospheric ozone column directly from a space-based instrument. This method is based on the physical differences in the Total Ozone Mapping Spectrometer (TOMS) measurement as a function of its scan-angle geometry. Tropospheric ozone in September-October exhibits a broad enhancement over South America, the southern Atlantic Ocean, and western South Africa and a minimum over the central Pacific Ocean. Tropical tropospheric ozone south of the equator is higher than north of the equator in September-October, the southern burning season. Conversely, ozone north of the equator is higher in March, the northern burning season. Overall, the ozone over the southern tropics during September-October is significantly higher than over the northern tropics. Abnormally high tropospheric ozone occurs over the western Pacific Ocean during the El Nino season when the ozone amounts are as high as the ozone over the Africa.

I. *Introduction*

Initial studies used a satellite technique for indirectly measuring tropospheric column ozone climatology by subtracting the average stratospheric-column ozone measured by the Stratospheric Aerosol and Gas Experiment (SAGE) from the total-column ozone climatology obtained from the Total Ozone Mapping Spectrometer (TOMS) (Fishman and Larsen, 1987). This technique is called the Tropospheric Ozone Residual (TOR) method. Two later studies, the Convective Cloud Differential (CCD) method (Ziemke et al., 1998) and the modified residual method (Hudson and Thompson, 1998), assumed that stratospheric ozone is invariant with longitude. As a result, these studies concluded the zonal variation of total ozone determines the zonal variation of tropospheric ozone in the tropics. However, Kim et al. (1996) suggested zonal wave 1 pattern in TOMS total ozone is due not only to tropospheric ozone but also to stratospheric ozone. The zonal structure of stratospheric ozone is still open to question.

Therefore, this study introduces the first method for determining the distribution of tropical tropospheric ozone directly from TOMS regardless of the zonal structure of stratospheric ozone. Furthermore, this study evaluates the existing methods for retrieving tropospheric ozone from satellite-based observation by comparing this independent method and the CCD

method with Measurements Of Pollution In The during March 2000 through April 2001.

II. Method

The TOMS instrument on board a sun-synchronous satellite measures UV radiances backscattered by the underlying atmosphere and Earth's surface or clouds (McPeters et al. 1996). TOMS scans its field of view (FOV) using a mirror perpendicular to the orbital track at 35 sample positions with 3-degree intervals. Scan positions 1, 18, and 35 correspond to highest scan position to the right, nadir, and highest scan position to the left, respectively. Hereafter, scan positions of 1, 2, 3, 33, 34, and 35 are defined as the high scan position, and scan positions of 16, 17, 18, 19, and 20 as the nadir scan position. The TOMS algorithm retrieves total ozone by comparing the measured radiances with calculated radiances at the determined parameters from a radiative transfer code. Then, the retrieved total ozone is either overestimated or underestimated depending on whether the assumed ozone amount below the effective scattering surface is less than or greater than the actual ozone amount. In order to analyze this error, Hudson et al. (1995) introduced a tropospheric ozone retrieval efficiency factor (TORE) relative to stratospheric ozone. Here, TORE is defined as the ratio of the calculated increase in N value by adding 10 DU to the troposphere to the increase in N value by adding 10 DU to the lower stratosphere. Here $N = -100 \log_{10} (A)$, where A is Earth's albedo at a given wavelength. Because the TORE is higher at nadir than at the high scan position, the retrieved total ozone at the nadir position is always closer to truth relative to the ozone at the high scan position. If the actual tropospheric ozone is less than the TOMS assumption, then the total ozone retrieved at the high scan positions will be greater than the ozone retrieved at the nadir position (i.e., the algorithm will not sense all of the negative deviation from the assumed amount). On the other hand, if the actual tropospheric ozone is greater than the TOMS assumption, then the retrieval at the high scan positions will be less than at the nadir retrieval (i.e., the algorithm will not sense all of the positive deviation from the assumed profile). Because the magnitude and sign of The differences between retrieved total ozone averaged over the high-scan positions and averaged over the nadir-scan positions (hereafter ΔO_3) depend on the difference between the actual and the assumed tropospheric ozone column, the distribution of tropospheric ozone can be determined directly from the difference between total ozone measurements at nadir and at the high scan position. The ΔO_3 values are related to the true changes in tropospheric ozone through the TORE, which itself is a function of viewing geometry and tropospheric ozone amount. The relationship is as follows:

$$\text{Tropospheric ozone column} = 32 + 6.7 \times \Delta O_3$$

Where 32 DU is TOMS tropical tropospheric ozone climatology and 6.7 is the efficiency scale factor.

III. Results

Figure 1 shows the distribution of tropical tropospheric ozone column derived from the scan-angel method (hereafter SAM) in September 1996. This distribution is consistent with the distribution of biomass burning activities. However, the distribution in this particular year is somewhat different from the climatological TOR results of Fishman and Brackett (1997) and the September 1997 CCD results of Ziemke et al. (1998). Figure 2 shows the distribution of tropospheric ozone derived from SAM in September 1997 corresponding to an El Nino season. A noticeable increase of very high column ozone occurs over the intense biomass burning over Malaysia, Indonesia, Borneo, and New Guinea. The distribution of enhanced ozone over northern equatorial Africa in March 1997

(Figure 3) is well correlated with the dry season north of the equator, strongly influencing biomass-burning activity. The enhanced ozone band migrates from the south of equatorial Africa to the north from September to March (Figure 1, 2, and 3). This movement agrees well with shifting from the southern biomass-burning season corresponding to the July-October period over the south to the northern burning season corresponding to the December-March period over the north. Because the CCD and modified residual methods rely heavily on the total ozone distribution, which maximizes south of the equator in Africa, these methods do not retrieve the enhanced tropospheric ozone in northern equatorial Africa seen by SAM in Figure 3 (Northern Africa Paradox). As a result, this method is able to derive the actual tropospheric enhancement in northern equatorial Africa in March 1997.

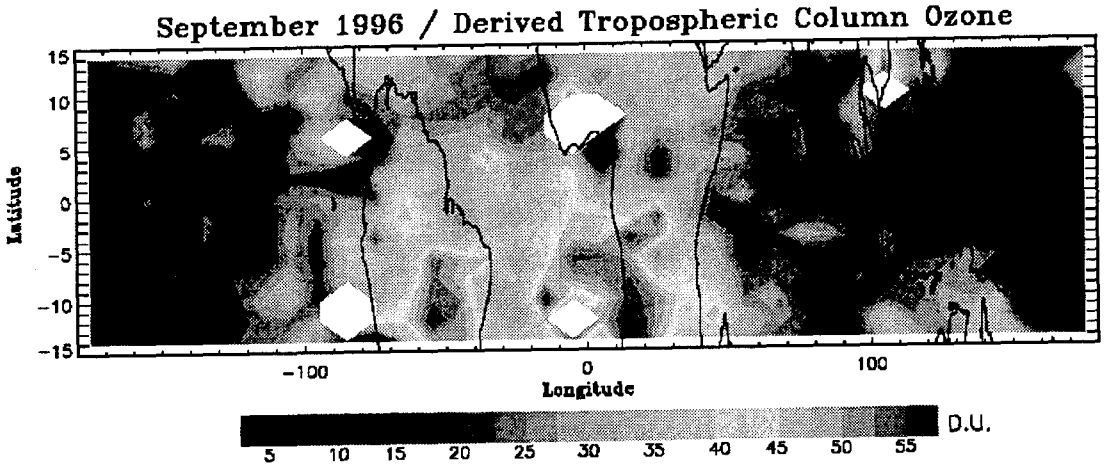

Fig. 1. Distribution of tropical tropospheric ozone in September 1996.

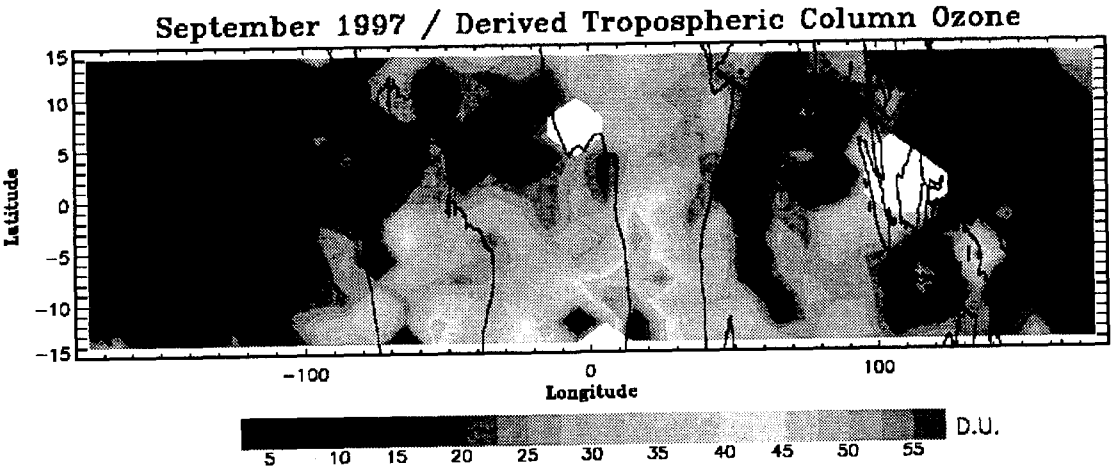

Fig. 2. Same as Figure 1, except for September 1997.

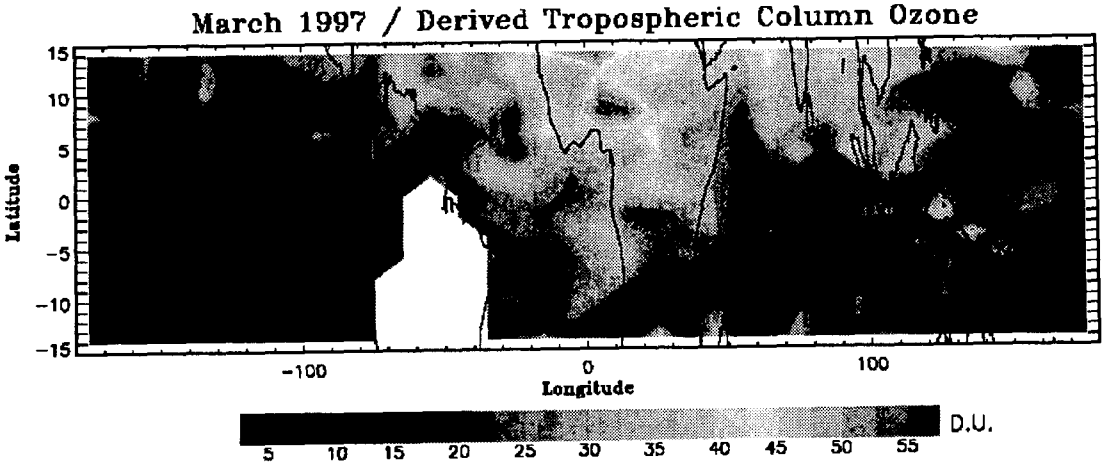

Fig. 3. Same as Figure 1, except for March 1997.

IV. Evaluation and Comparison

Tropospheric ozone derived from CCD method reflects photochemical effect, such as biomass burning (Ziemke et al., 1998). In order to investigate photochemical effect on tropospheric ozone, this study utilizes carbon monoxide from MOPITT as photochemical proxy of tropospheric ozone. The distribution of MOPITT CO measurements agrees well with the distribution of tropospheric ozone derived from SAM and CCD method in the tropics during September through November 2000. The CCD results show the enhanced ozone over the south Atlantic in SON, the southern burning season. Also the SAM results presents higher ozone corresponding with increases in biomass burning in the south Atlantic during the same period. The distribution of SAM tropospehric ozone is similar to MOPITT CO measurements during December 2000 through February 2001, the northern burning season. However, in DJF, the distribution of tropospheric ozone derived from CCD method does not show higher ozone related to biomass burning over the northern Africa. The influence of biomass burning in the SAM results is clearly seen in the seasonally enhanced ozone.

The SAM results are correlated with MOPITT CO between 10S and 10N. There is also a relationship between MOPITT CO measurements and tropospheric ozone derived from CCD method. We expect that the correlation between CCD tropospheric ozone and MOPITT CO is higher than the correlation between SAM tropospheric ozone and MOPITT CO because the CCD method assumed tropospheric ozone resulting from photochemical production. However, the correlation between the CCD results and MOPITT CO does not show better relationship than the correlation between SAM results and MOPITT CO from March 2000 to April 2001. The correlation between CCD tropospheric ozone and MOPITT CO is better than the correlation between the SAM results and CO especially in the austral dry season. On the contrary, the correlation between SAM tropospheric ozone and MOPITT CO is better than the correlation between the CCD results and CO in the boreal dry season.

In conclusion, the correlation between tropospheric ozone derived from SAM and CCD method is good. Despite the differences in the techniques there is a good agreement. Tropospheric ozone derived from SAM is identical to tropospheric ozone derived from CCD method. However, the SAM maps can resolve the Northern African Paradox that is persistent in the CCD maps.

References

Fishman, J., and J. C. Larsen, 1987, Distribution of total ozone and stratospheric ozone in the tropics: Implications for the distribution of tropospheric ozone, J. Geophys. Res., 92: 6627-6634.

Fishman, J, and V. G. Brackett, 1997, The climatological distribution of tropospheric ozone derived from satellite measurements using version 7 Total Ozone Mapping Spectrometer and Stratospheric Aerosol and Gas Experiment data sets. J. Geophys. Res., 102: 19,275-19,278.

Hudson, R. D., J.-H. Kim, and A. M. Thompson, 1995, On the derivation of tropospheric column from radiances measured by the total ozone mapping spectrometer, J. Geophys. Res., 100: 11,137-11,145.

Hudson, R. D., and A. M. Thompson, 1998, Tropical tropospheric ozone from total ozone mapping spectrometer by a modified residual method, J. Geophys. Res., 103: 22,129-22,145.

Kim, J. H., and M. J. Newchurch, 1996, Climatology and trends of tropospheric ozone over the eastern Pacific Ocean: The influences of biomass burning and tropospheric dynamics, Geophys. Res. Lett., 23: 3723-3726.

McPeters, R. D., and Coauthors, 1996, Nimbus-7 Total Ozone Mapping Spectrometer (TOMS) Data Products User's Guide, NASA, 67.

Ziemke, J. R., S. Chandra, and P. K. Bhartia, 1998, Two new methods for deriving tropospheric column ozone from TOMS measurements: Assimilated UARS MLS/HALOE and convective-cloud differential techniques, J. Geophys. Res., 103: 22,115-22,127.